Magnetic Nanoparticle Assembly on Surfaces Using Click Chemistry

Sachin Kinge,*[†] Tian Gang,[‡] Wouter J. M. Naber,[‡] Wilfred G. van der Wiel,*[‡] and
David N. Reinhoudt[†]

[†]*Laboratory of Supramolecular Chemistry and Technology and* [‡]*NanoElectronics Group, MESA*[+] *Institute for Nanotechnology, University of Twente, P.O. Box 217, 7500 AE Enschede, The Netherlands*

Controlled assembly of ferromagnetic nanoparticles on surfaces is of crucial importance for a range of spintronic and data storage applications. Here, we present a novel method for assembling monolayers of ferromagnetic FePt nanoparticles on silicon oxide substrates using "click chemistry". Reaction of alkyne-functionalized FePt nanoparticles with azide-terminated self-assembled monolayers (SAMs), on silicon oxide, leads to the irreversible attachment of magnetic nanoparticles to the surface via triazole linkers. Based on this covalent interaction, well-packed monolayers of FePt nanoparticles were prepared and nanoparticle patterns are generated on surfaces via microcontact printing (μCP).

Ferromagnetic nanoparticles are very promising for creating ultrasmall devices for spintronics, magnetic sensing, and ultrahigh density data storage.[1-5] In this regard monodisperse FePt nanoparticles are very interesting; their synthesis and characterization are extensively studied.[1,6-9] After annealing, they show ferromagnetic behavior up to room temperature due to their very high magnetocrystalline anisotropy ($K_u = 7 \times 10^6$ J/m^3). They therefore have higher chemical stability compared to Co-based data storage materials.[8-10] Instead of multiple grains for the storage of one bit of information, FePt nanoparticles allow for one bit per grain, enabling terabit/in.^{2} storage capacity.[10] However, for practical applications, a regularly assembled nanoparticle array is a prerequisite. Self-assembly of nanoparticles on surfaces is very attractive for this purpose. So far, only a few self-assembly methods have been reported to organize magnetic nanoparticles, like drying-mediated assembly, layer-by-layer assembly via electrostatic interactions, and the coupling via amino-terminated APTS [3-(2-aminoethlyamino)propyl]trimethoxysilane, which replaces the surfactants that stabilize the nanoparticles.[11-15] These methods have several drawbacks, such as instability or nonspecific particle–surface interactions.

Here, we present "click chemistry" as an alternative method to assemble monolayers of FePt nanoparticles via specific particle–substrate interactions. Click chemistry is very useful tool for creating new materials based on highly selective and quantitative coupling reactions, in particular the Huisgen 1,3-dipolar cycloaddition of azides and alkynes to form 1,2,3-triazoles.[16-23] The copper(I)-catalyzed azide–alkyne cycloaddition reactions proceed with high yields and without byproducts.[24,25] This method

(1) Hyeon, T. Chemical synthesis of magnetic nanoparticles. *Chem. Commun.* **2003**, 927–934.
(2) Jeong, U.; Teng, X. W.; Wang, Y.; Yang, H.; Xia, Y. N. Superparamagnetic Colloids: Controlled Synthesis and Niche Applications. *Adv. Mater.* **2007**, *19*, 33–60.
(3) Tartaj, P.; Morales, M. P.; Gonzalez-Carreno, T.; Veintemillas-Verdaguer, S.; Serna, C. J. Advances in magnetic nanoparticles for biotechnology applications. *J. Magn. Magn. Mater.* **2005**, *290*, 28–34.
(4) Hadjipanayis, G. C.; Marinescu, M.; Huang, Y. H.; Bonder, M. J.; Gabay, A. Magnetic Meta-Materials for High-Technology Applications. *Sens. Lett.* **2007**, *5*, 1–9.
(5) Naber, W. J. M.; Faez, S.; Van der Wiel, W. G. Organic spintronics. *J. Phys. D: Appl. Phys.* **2007**, *40*, 205–228.
(6) Hernando, A.; Crespo, P.; Garcia, M. A. Metallic Magnetic Nanoparticles. *TheScientificWorld* **2005**, *5*, 972–1001.
(7) Kang, S. S.; Miao, G. X.; Shi, S.; Jia, Z.; Nikles, D. E.; Harrell, J. W. Enhanced Magnetic Properties of Self-Assembled FePt Nanoparticles with MnO Shell. *J. Am. Chem. Soc.* **2006**, *128*, 1042–1043.
(8) Kang, S. S.; Shi, S.; Miao, G. X.; Jia, Z.; Nikles, D. E.; Harrell, J. W. Synthesis and Magnetic Properties of FePt Nanoparticles with Hard Nonmagnetic Shells. *J. Nanosci. Nanotechnol.* **2007**, *7*, 350–355(6).
(9) Rellinghaus, B.; Stappert, S.; Acet, M.; Wassermann, E. F. Magnetic properties of FePt nanoparticles. *J. Magn. Magn. Mater.* **2003**, *266*, 142–154.
(10) Terris, B. D.; Thomson, T. Nanofabricated and self-assembled magnetic structures as data storage media. *J. Phys. D: Appl. Phys.* **2005**, *38*, R199–222.
(11) Schrefl, T.; Hrkac, G.; Suess, D.; Scholz, W.; Fidler, J. Coercivity and remanence in self-assembled FePt nanoparticle arrays. *J. Appl. Phys.* **2003**, *93*, 7041–7043.
(12) Acet, M.; Mayer, C.; Muth, O.; Terheiden, A.; Dyker, G. Formation of extended ordered monolayers of FePt nanoparticles. *J. Cryst. Growth* **2005**, *285*, 365–371.
(13) Sun, S. H.; Anders, S.; Hamann, H. F.; Thiele, J. U.; Baglin, J. E. E.; Thomson, T.; Fullerton, E. E.; Murray, C. B.; Terris, B. D. Polymer mediated self-assembly of magnetic nanoparticles. *J. Am. Chem. Soc.* **2002**, *124*, 2884–2885.
(14) Sun, S. H.; Anders, S.; Thomson, T.; Baglin, J. E. E.; Toney, M. F.; Hamann, H. F.; Murray, C. B.; Terris, B. D. Controlled Synthesis and Assembly of FePt Nanoparticles. *J. Phys. Chem. B* **2003**, *107*, 5419–5425.
(15) Yu, A. C. C.; Mizuno, M.; Sasaki, Y.; Inoue, M.; Kondo, H.; Ohta, I.; Djayaprawira, D.; Takahashi, M. Fabrication of monodispersive FePt nanoparticle films stabilized on rigid substrates. *Appl. Phys. Lett.* **2003**, *82*, 4352–4354.
(16) Nandivada, H.; Jiang, X. W.; Lahann, J. Click Chemistry: Versatility and Control in the Hands of Materials Scientists. *Adv. Mater.* **2007**, *19*, 2197–2208.
(17) Binder, W. H.; Kluger, C. Azide/Alkyne-"Click" Reactions: Applications in Material Science and Organic Synthesis. *Curr. Org. Chem.* **2006**, *10*, 1791–1815.
(18) Binder, W. H.; Sachsenhofer, R.; Straif, C. J.; Zirbs, R. Surface-modified nanoparticles via thermal and Cu(i)- mediated "click" chemistry: generation of luminescent CdSe nanoparticles with polar ligands guiding supramolecular recognition. *J. Mater. Chem.* **2007**, *17*, 2125–2132.
(19) Brennan, J. L.; Hatzakis, N. S.; Tshikhudo, T. R.; Dirvianskyte, N.; Razumas, V.; Patkar, S.; Vind, J.; Svendsen, A.; Nolte, R. J. M.; Rowan, A. E.; Brust, M. Bionanoconjugation via Click Chemistry: The Creation of Functional Hybrids of Lipases and Gold Nanoparticles. *Bioconjugate Chem.* **2006**, *17*, 1373–1375.
(20) Fournier, D.; Hoogenboom, R.; Schubert, U. S. Clicking polymers: a straightforward approach to novel macromolecular architectures. *Chem. Soc. Rev.* **2007**, *36*, 1369–1380.
(21) Gil, M. V.; Arevalo, M. J.; Lopez, O. Click Chemistry - What's in a Name? Triazole Synthesis and Beyond. *Synthesis* **2007**, *11*, 1589–1620.
(22) Lummerstorfer, T.; Hoffmann, H. Click Chemistry on Surfaces: 1,3-Dipolar Cycloaddition Reactions of Azide-Terminated Monolayers on Silica. *J. Phys. Chem. B* **2004**, *108*, 3963–3966.
(23) Moses, J. E.; Moorhouse, A. D. The growing applications of click chemistry. *Chem. Soc. Rev.* **2007**, *36*, 1249–1262.
(24) Narayan, S.; Muldoon, J.; Finn, M. G.; Fokin, V. V.; Kolb, H. C.; Sharpless, K. B. On Water": Unique Reactivity of Organic Compounds in Aqueous Suspension. *Angew. Chem., Int. Ed.* **2005**, *44*, 3275–3279.
(25) Rodionov, V. O.; Fokin, V. V.; Finn, M. G. Mechanism of the Ligand-Free Cu^I-Catalyzed Azide-Alkyne Cycloaddition Reaction. *Angew. Chem., Int. Ed.* **2005**, *44*, 2210–2215.

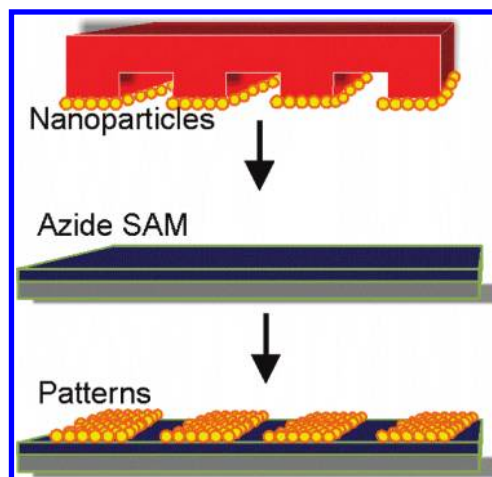**Scheme 1. Assembling Ferromagnetic FePt Nanoparticles as SAM Using Click Chemistry**

Scheme 2. Patterning FePt Nanoparticles via μCP Based on Click Chemistry
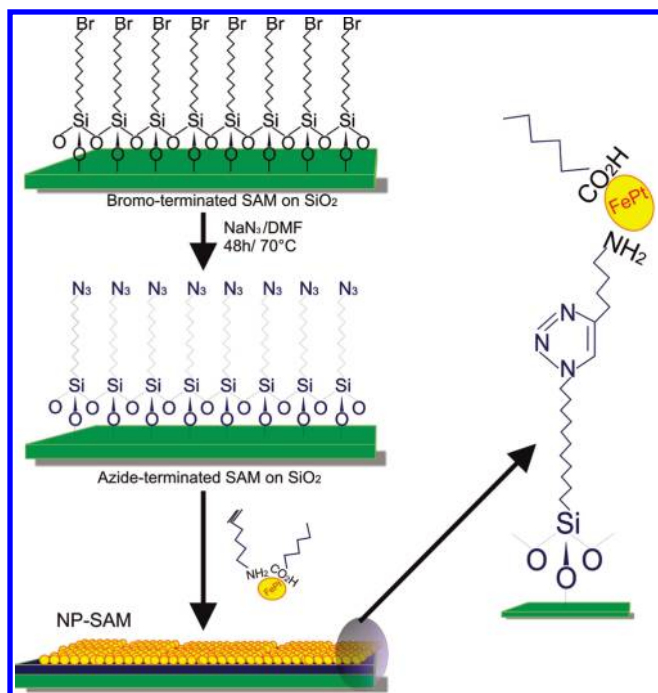
has been used for a variety of applications such as functionalization of polymers, biomolecules, bulk surfaces, etc.[17−26] Previously, Fleming et al.,[27] White et al.,[28] Lin et al.,[29] and Binder et al.[30] have reported the functionalization of gold, iron oxide, or CdSe nanoparticles using click chemistry. In our group previously we have exploited this approach to create molecular nanostructures on surfaces.[31]

Here, we describe click chemistry to link (ferromagnetic) nanoparticles to substrate surfaces. To the best of our knowledge, this is the first example of assembling and attaching nanoparticles on a surface using click chemistry.

Results and Discussion

The FePt nanoparticles were synthesized according to Sun's method.[14] Subsequently, the oleic acid and oleylamine groups at the surface of the nanoparticles were replaced by 5-hexanoic acid and 6-amino-1-hexyne groups to form alkyne-substituted FePt nanoparticles. These nanoparticles were assembled (Scheme 1) or patterned (Scheme 2) on the substrate by reaction with azide-terminated SAMs on silicon oxide substrates.

The nanoparticle monolayers and patterned structures were annealed under N_2 protection at 700 °C to transform the nanoparticles from the paramagnetic chemically disordered FCC phase

to the ferromagnetic ordered $L1_0$ phase. Magnetic hysteresis were recorded by a vibrating sample magnetometer (VSM) to confirm this phase transformation and the ferromagnetic behavior of the nanoparticles.

TEM analysis of FePt nanoparticles functionalized with 6-amino-1-hexyne and 5-hexanoic acid indicated monodisperse nanoparticles of 5 ± 0.5 nm size (Figure 1). These nanoparticles are redispersed in hexane. Based on XRD analyses, the elemental composition was $Fe_{48}Pt_{52}$.

Azide-terminated SAMs were prepared in situ from 11-bromoundecylsiloxane SAMs to assemble or to create FePt nanoparticle patterns on the silicon oxide substrates. The azide-terminated SAMs were subsequently reacted with alkyne-terminated FePt nanoparticles according to Scheme 1. The exchange of the surface bromine group of 11-bromoundecylsiloxane SAMs against azide via nucleophilic substitution with DMF solution of sodium azide proceeded quantitatively and is accompanied in the infrared spectra by an intense $\nu(N_3)$ absorption at 2014 cm^{-1} corresponding to the asymmetric stretch (Figure 2). The XPS spectrum of the bromo-terminated SAMs shows a pronounced Br(3d) peak at 70.5 eV (Figure 2). After substitution with NaN$_3$, the Br(3d) peak disappeared and an N(1s) peak appeared at 400 eV, which confirmed complete reaction. Ellipsometry showed that the bromo SAM has a thickness $d = 1.34 \pm 0.08$ nm and the azido SAM $d = 1.48 \pm 0.10$ nm, in agreement with the previous reported values.[22,30]

To create a monolayer of FePt nanoparticles on silicon oxide substrate, the azide-terminated substrates were immersed in the alkyne-functionalized nanoparticle solution (DMSO:H_2O; 4:1) for 15 min. $CuSO_4 \cdot 5H_2O$ and sodium ascorbate were subsequently added to the solution to catalyze the reaction. Then the mixture was stirred for 48 h at RT.[30] The substrates were removed and washed with ethanol to remove any physisorbed layer of nanoparticles.

The μCP was carried out with and without Cu(I) catalysts, and no significant differences were observed. As we have previously reported, during μCP high local concentration of functional groups can give click reactions without the need for catalysts.[30] To discriminate whether the particles are attached to the surface through physisorption or specific covalent reactions, a similar nanoparticle deposition was repeated on a bare substrate. In addition, non-alkyne-functionalized FePt nanoparticles (oleic acid and oleylamine stabilized) were also deposited on the azide-terminated substrates. The absence of nanoparticles in both cases

(26) Hawker, C. J.; Wooley, K. L. The Convergence of Synthetic Organic and Polymer Chemistries. *Science* **2005**, *309*, 1200–1205.

(27) Fleming, D. A.; Thode, C. J.; Williams, M. E. Triazole Cycloaddition as a General Route for Functionalization of Au Nanoparticles. *Chem. Mater.* **2006**, *18*, 2327–2334.

(28) White, M. A.; Johnson, J. A.; Koberstein, J. T.; Turro, N. J. Clickable" Agarose for Affinity Chromatography. *J. Am. Chem. Soc.* **2006**, *128*, 11356–11357.

(29) Lin, P.-C.; Ueng, S.-H.; Yu, S. C.; Jan, M.-D.; Adak, A. K.; Yu, C. C.; Lin, C.-C. Surface Modification of Magnetic Nanoparticle via Cu(I)-Catalyzed Alkyne-azide [2 + 3] Cycloaddition. *Org. Lett.* **2007**, *9*, 2131–2134.

(30) Binder, W. H.; Lomoschitz, M.; Sachsenhofer, R.; Friedbacher, G. Reversible and Irreversible Binding of Nanoparticles to Polymeric Surfaces. *J. Nanomater.* **2009**, ID 613813

(31) Rozkiewicz, D. I.; Janczewski, D.; Verboom, W.; Ravoo, B. J.; Reinhoudt, D. N. Click" Chemistry by Microcontact Printing. *Angew. Chem., Int. Ed.* **2006**, *45*, 5292–5296.
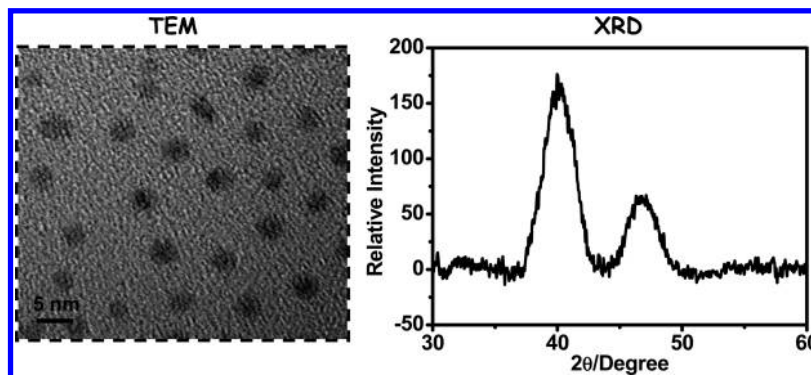
Figure 1. TEM micrograph of 5 ± 0.5 nm $Fe_{52}Pt_{48}$ nanoparticles stabilized with 6-amino-1-hexyne and 5-hexanoic acid (left) and XRD pattern of the as synsesized nanoparticles (right).
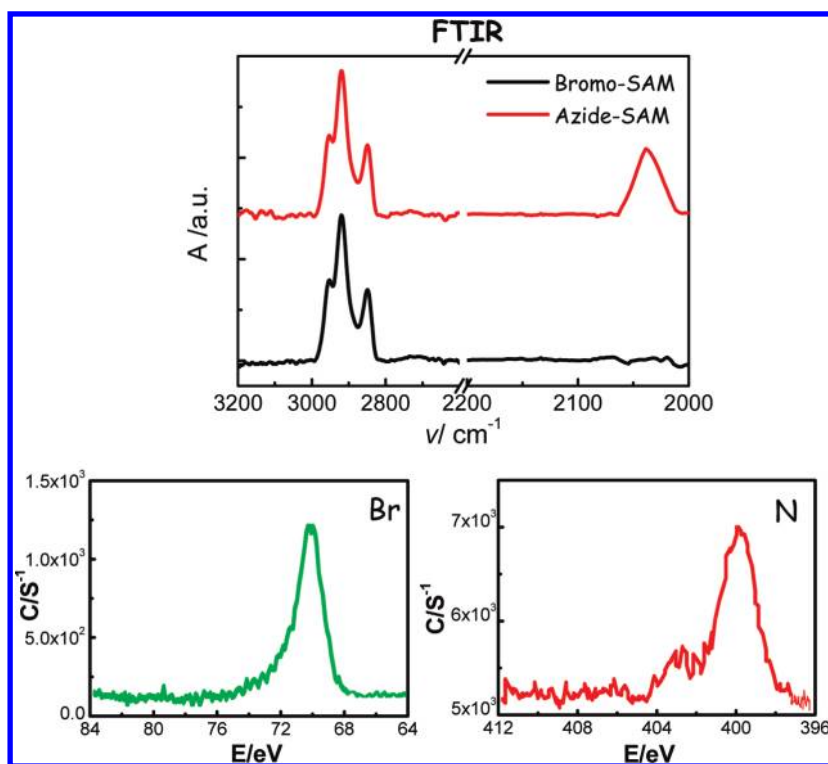

Figure 2. FTIR spectra of bromo-terminated and azide-terminated SAMs on the silicon oxide substrates; XPS analysis showing the presence of Br and N in the respective SAMs.

clearly confirms that nanoparticles are attached through the triazole formation between the alkyne-functionalized nanoparticles and azide-terminated substrate. (XPS and FTIR analyses cannot be performed in addition to monitoring the triazole formation, as most of the nanoparticle surface is still covered with an alkyne-functionalized layer with presumably only few of the groups replaced by triazoles due to spherical geometry of the nanoparticles.)

SEM micrographs of the nanoparticle SAMs show good coverage all over the substrate surface (Figure 3). SEM analysis (Figure 4) on the linear patterns of the nanoparticles showed 10 μm arrays of nanoparticles separated by 5 μm distances over the substrate.

VSM measurements confirmed magnetic hysteresis for both the full nanoparticle SAMs and the patterned nanoparticle SAMs after annealing at 700 °C under N_2 protection, indicating the ferromagnetic character of the particles at room temperature (Figure 5). The ratio of magnetization between full nanoparticle SAMs and the patterned nanoparticle SAMs is about 1.25, which is slightly lower than the volume ratio of 1.5. This may due to a small variation in substrate size and or the packing density of the nanoparticles. A larger coercivity is observed in case of a fully covered FePt monolayer compared to the patterned FePt monolayer. This indicates an improved chemical ordering, which translates into enhanced magnetocrystalline anisotropy. As shown above, the packing density of fully covered FePt monolayer is higher than the patterned FePt monolayer. Annealing process leads to a higher degree of agglomeration, and the agglomerated particles have a larger size and thus a better chemical ordering.[32,33]

(32) Schrefl, T.; Hrkac, G.; Suess, D.; Scholz, W.; Fidler, J. Coercivity and remanence in self-assembled FePt nanoparticle arrays. *J. Appl. Phys.* **2003**, *93*, 7041–7043.
(33) Lu, H. M.; Cao, Z. H.; Zhao, C. L.; Li, P. Y.; Meng, X. K. Size-dependent ordering and Curie temperatures of FePt nanoparticles. *J. Appl. Phys.* **2008**, *103*, 123526–123526-4.

Conclusions

Click chemistry can be applied to assemble magnetic nanoparticles onto azido-terminated silicon oxide substrates. Monolayers of the nanoparticles were obtained using copper(I)-catalyzed click reaction. Further, we envisage that noncatalyzed click chemistry between alkyne-functionalized nanoparticles and azide-terminated SAMs coupled with μCP can generate well-defined nanoparticles patterns. This methodology has potential for data storage and spintronics applications.

Experimental Section

Synthesis of Alkyne-Terminated FePt Nanoparticles. Alkyne-terminated FePt nanoparticles were synthesized via a modified Sun's method.[14] A solution of 0.25 mmol of Pt(acac)$_2$ and 0.75 mmol of 1,2 hexadecanediol in 20 mL of octyl ether was heated to 80 °C. To this solution 0.5 mmol of oleic acid, 0.5 mmol of oleylamine, and 0.5 mmol of iron pentacarbonyl were added via a syringe. This mixture was further heated to 150 °C for 1 h. The black product was precipitated using ethanol, and particles were redispersed in hexane. Replacement of oleic acid and oleyl amine groups by 5-hexanoic acid and 6-amino-1-hexyne was achieved as described by White et al.[28] First, oleic acid and oleylamine were stripped off from the nanoparticles by washing with ethanol, collecting the black precipitate, and redispersing in hexane (3 times). After washing, the nanoparticles are no longer soluble in hexane, indicating complete removal of the oleic acid and oleylamine from the nanoparticles surfaces. This was verified by FTIR, which showed complete absence of oleic acid and oleylamine. Subsequently, the nanoparticles were subjected to ultrasonication for 30 min with 5-hexanoic acid and 6-amino-1-hexyne (1:1:1 wt %
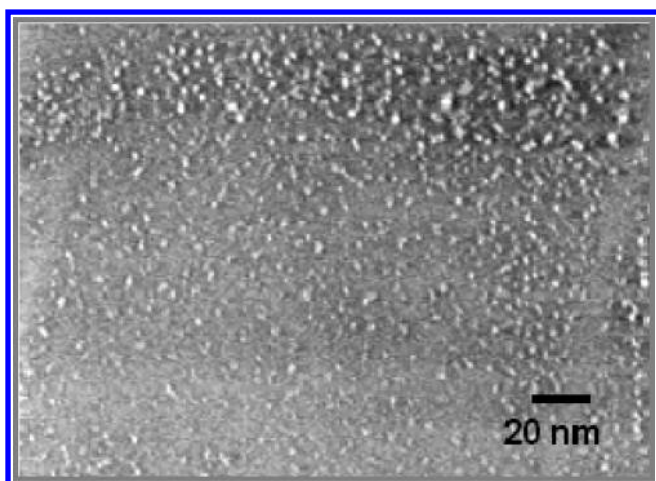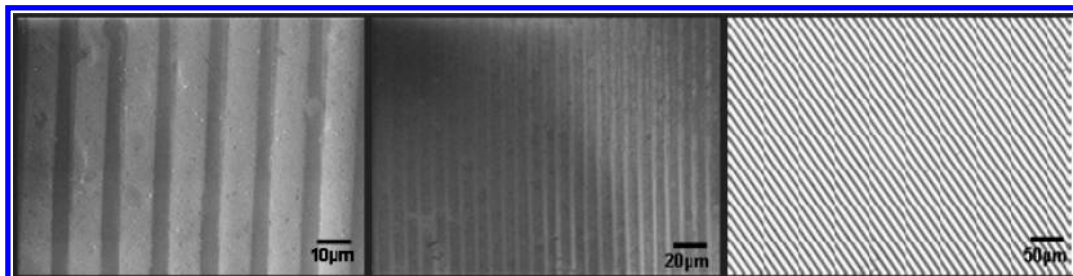
ratio of FePt:5-hexanoic acid 6-amino-1-hexyne) in hexane. Particle sizes were analyzed by TEM (Philips CM-30 Twin operating at 200 kV voltage). A drop of hexane solution of the nanoparticles was deposited on a carbon-coated copper grid. ^{1}H NMR spectra were recorded in *d*-DMSO on a Varian Unity 300 locked to the deuterated solvent at 300.1 MHz. NMR showed presence of both 5-hexanoic acid and 6-amino-1-hexyne in the appropriate ratio. The nanoparticle sample was analyzed by powder X-ray diffraction (XRD) analysis using a PHILIPS X'Pert diffractometer (Cu Kα, λ = 1.5418 Å).

Preparation of 11-Azidoundecyl Monolayer on Silicon Oxide (Scheme 1). N$_3$ (azide)-terminated monolayers on silicon oxide were obtained according to the methodology previously described.[22,30] The p-doped, (100)-oriented silicon wafers (Gritek, prime grade, 7−21 Ω cm specific resistivity, 0.5 mm thickness) were cut into 10 × 10 mm^2 pieces. First, the silicon wafers were sonicated in ethanol and blow-dried under nitrogen. In order to remove hydrocarbon contaminants and to generate a native oxide layer on the substrate surface, wafers were activated by 15 min exposure to a UV/ozone atmosphere in a plasma oxidation setup (Boekel Industries). Subsequently, the substrates were immersed in a 1 mM toluene solution of 11-bromoundecyltrichlorosilane for 45 min at room temperature. The wafers were rinsed with toluene, acetone, and ethanol to remove any physisorption. This generates a bromo-terminated monolayer on the silicon oxide substrate. In the next step, substitution of the bromo-terminated monolayer with NaN$_3$ leads to the formation of azide (N$_3$)-terminated monolayers on the substrate. This was achieved by immersing the substrates in a saturated sodium azide solution (NaN$_3$) in DMF for 48 h at 70 °C, followed by rinsing with water and ethanol.

Ellipsometric thicknesses were measured with a PLASMOS SD7.01I ellipsometer. Optical constants of $n = 3.865$ and $k = 0.019$ for Si, $n = 1.465$ and $k = 0$ for SiO$_2$, and $n = 1.50$ and $k = 0$ for the organic films were used. Raster scans were performed of 25 points per wafer, and their values were averaged.

Grazing angle infrared spectra (*GAIS*) of the SAMs were recorded on a BioRad FTS-60A spectrometer with a liquid nitrogen cooled cryogenic, external mercury cadmium telluride (MCT) detector with its sample area modified to accommodate external reflection sample geometry. The sample area is maintained under nitrogen, and spectra were recorded in zthe mid-IR region (1024 scans) at 4 cm^{-1} resolution 20 kHz speed.

Figure 3. SEM micrographs of FePt nanoparticles assembled as a monolayer on the azide-terminated silicon oxide substrates captured from different regions. It shows the attachment of nanoparticles on the surface of the substrate.
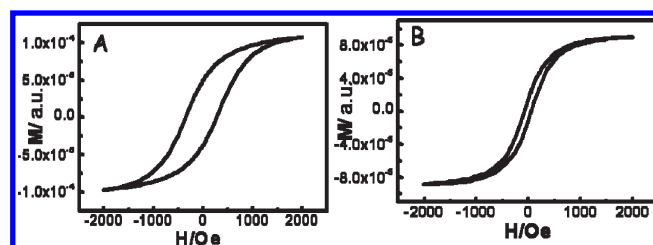

Figure 5. VSM magnetization measurements of FePt nanoparticles in a full SAM (A) and a line patterned SAM (B) on the silicon oxide substrate at RT after annealing at 700 °C under N$_2$ protection.

Figure 4. Optical micrograph of FePt nanoparticle arrays formed on the silicon oxide substrate by μCP. Parallel lines of 10 μm are placed 5 μm apart. Well-patterned layers of FePt nanoparticles are observed.

XPS measurements were performed with Physical Electronics Quantum 2000 equipment, equipped with a spherical sector analyzer and a multichannel plate detector. For the survey scan the pass energy was 117 eV, the X-ray beam was set to high power mode (100 W/100 μm), and the diameter beam scanned over a 1000 μm × 500 μm area. For element scans the pass energy was 29.35 eV, the X-ray beam was set to 25 W/100 μm, and the diameter beam scanned over a 1000 μm × 500 μm area. The excitation source was Al Kα monochromatic radiation with a source energy = 1486.6 eV. The takeoff angle (analyzer angle-to-sample surface) was set to 30°. The temperature during the analysis was 298 K, and the pressure was between 1 and 3×10^{-8} Torr (argon pressure for charge control). For atomic concentration the Shirley background subtraction was employed. The sensitivity factors were provided by Physical Electronics Multipack software version 6.1A. As a reference for surface charging the hydrocarbon C 1s signal at 284.8 eV was used.

Magnetic studies were carried out using a DMS vibrating sample magnetometer (model VSM10) with fields up to 1500 kA/m and a sensitivity of 10^{-6} mAm^2. Measurements were done on both nanoparticles assemblies and patterned nanoparticles on oxidized silicon substrates.

Assembly and Pattering of FePt Nanoparticles on SiO$_2$ (Scheme 1). FePt nanoparticles (250 mg) were added to 5 mL of DMSO:H$_2$O (4:1), CuSO$_4$·5H$_2$O (62 mg), and sodium ascorbate (81 mg) and deposited on top of the azide-modified substrate. Stirring for 48 h at RT was followed.[30] The substrate was removed and washed with ethanol to remove the physisorbed layer of nanoparticles. The resulting layer was analyzed with scanning electron microscopy (SEM), performed with a JEOL 5610 apparatus. Samples for transmission electron microscopy (TEM) were prepared by deposition and evaporation of a drop of a solution in chloroform onto amorphous graphite. Linear patterns of nanoparticles were obtained by μCP as described below.

Microcontact Printing of Nanoparticles. Stamps were fabricated by casting a 10:1 (v/v) mixture of PDMS and curing agent (Sylgard 184, Dow Corning) against a photolithographically patterned silicon master, cured for 1 h at 60 °C, and released at this curing temperature to avoid buildup of tension due to thermal shrinkage. PDMS stamps, used for μCP, were left in the oven at 60 °C for at least 18 h to ensure complete curing. Subsequently, the stamps were inked by immersion into the adsorbate solution of nanoparticles (DMSO:H$_2$O; 4:1) for 15 min. After withdrawal from the solution and drying under a continuous stream of nitrogen for 1 min, the stamps were applied with conformal contact for 5 min on the azide SAMs. Reinking was done after each printing step. This process was carried out without using any Cu(I) catalyst. Finally, the substrates were systematically rinsed with water and ethanol.